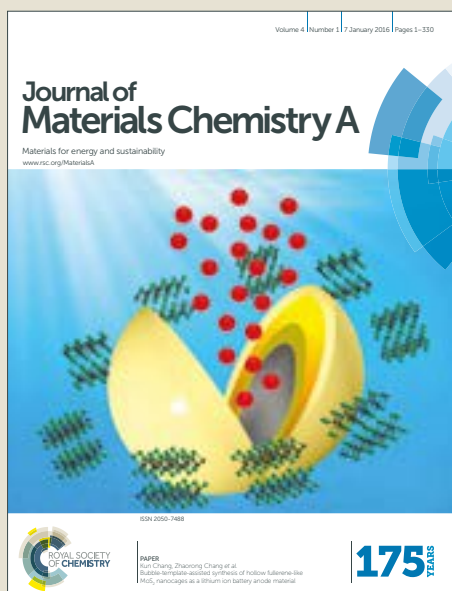


# Journal of Materials Chemistry A

Accepted Manuscript



This article can be cited before page numbers have been issued, to do this please use: C. Su, H. he, L. xu, K. Zhao, C. Zheng and C. zhang, *J. Mater. Chem. A*, 2017, DOI: 10.1039/C6TA10127E.



This is an Accepted Manuscript, which has been through the Royal Society of Chemistry peer review process and has been accepted for publication.

Accepted Manuscripts are published online shortly after acceptance, before technical editing, formatting and proof reading. Using this free service, authors can make their results available to the community, in citable form, before we publish the edited article. We will replace this Accepted Manuscript with the edited and formatted Advance Article as soon as it is available.

You can find more information about Accepted Manuscripts in the [author guidelines](#).

Please note that technical editing may introduce minor changes to the text and/or graphics, which may alter content. The journal's standard [Terms & Conditions](#) and the ethical guidelines, outlined in our [author and reviewer resource centre](#), still apply. In no event shall the Royal Society of Chemistry be held responsible for any errors or omissions in this Accepted Manuscript or any consequences arising from the use of any information it contains.



## Mesoporous conjugated polymer based on high free radical density polytriphenylamine derivative: its preparation and electrochemical performance as cathode material for Li-ion batteries

Received 00th January 20xx,  
Accepted 00th January 20xx

DOI: 10.1039/x0xx00000x

www.rsc.org/

Chang Su,<sup>b,a\*</sup> Huihui He,<sup>c</sup> Lihuan Xu,<sup>b</sup> Kai Zhao,<sup>c</sup> Chuncui Zheng<sup>c</sup> and Cheng Zhang<sup>a,\*</sup>

A novel mesoporous conjugated polymer-Poly(4,4',4''-tris(N,N-diphenyl-amino) triphenylamine) (PTDATA), which was one of polytriphenylamine derivatives with high free radical density, has firstly been prepared by chemical oxidative polymerization. Compared to polytriphenylamine (PTPA) with aggregated morphology and relatively low surface area (5.6 m<sup>2</sup>/g), PTDATA exhibited a nanofibers-packed mesoporous structure with obviously improved surface area of 560.58 m<sup>2</sup>/g. When explored as the cathode material for organic free radical batteries, PTDATA showed a well-defined multistage discharge voltage plateau and an improved capacity of 133.1 mAh/g, which was equal to 92.8 % of its theoretical capacity (143.5 mAh/g). Also, PTDATA exhibited an enhanced rate performance of 125.4, 114.1, 97.5 and 90.9 mAh/g with a 10 times increase of the current density from 50 to 500 mA/g, respectively. The excellent electrochemical performances of the PTDATA electrode were due to its special chemical structure of high free radical density and its high specific surface caused by the nanofibers-packed mesoporous morphology, which made PTDATA be a good potential candidate as the organic cathode materials for high-performance organic lithium secondary batteries.

### Introduction

Nowadays, lithium ion batteries as a promising power source have been widely used in electronic devices such as cell phones and laptop computers.<sup>1-3</sup> However, the commonly used cathode materials in state-of-the-art lithium ion batteries are generally inorganic materials (e.g., LiCoO<sub>2</sub>), which suffer from some drawbacks involving the limited theoretical capacities, the limited mineral resources and the large energy consumption during synthesis.<sup>4-8</sup> Furthermore, the demands for high capacity also limit their large scale applications for upcoming electric vehicles (EVs) and renewable power stations.<sup>4, 9</sup> To meet increasing demands of green and sustainable electric power storage, organic electrode materials have recently attracted considerable attention because of their potential high redox capacity, resource abundance, environmental friendliness and structural diversion.<sup>10,11</sup> A number of organic compounds have been investigated as novel energy storage materials for the positive electrode of

lithium batteries, which mainly include organic conductive polymers (polyaniline, polythiophene and polyimide),<sup>12, 13</sup> organosulfur compounds,<sup>14</sup> carbonyl-based compounds<sup>15-17</sup> and stable radical polymers,<sup>18,19</sup> et al.

Among them, polytriphenylamine (PTPA) as well as its derivatives, as a kind of radical polymer, has been explored recently as the electrode materials in the energy storage field, such as lithium ion batteries and super capacitors,<sup>20-25</sup> due to their excellent charge transport, thermal and morphological stabilities, and electroluminescence. As reported,<sup>25</sup> PTPA, composed of a p-conjugated triphenylamine substructure, showed good electrochemical performance and well-defined voltage plateaus (~3.6 V) as the cathode of lithium ion batteries, which could contribute to the reversible redox radicals nature of PTPA. However, the limited theoretical capacity of PTPA (109 mAh/g), which is lower than that of the commercial LiCoO<sub>2</sub> (about 140 mAh/g), hinder its further research in the future. According to the formula of the theoretical specific capacity:  $C_t$  (mAh/g) =  $n \times F / M_w$ , in which  $C_t$ ,  $n$ ,  $F$  and  $M_w$  respectively mean the theoretical specific capacity, the transferred electron number in each structural unit, the Faraday constant and the molecular weight of the structural unit, there are two ways to improve the theoretical capacity of an organic electrode material: one is adopting multi-electron reactions and another is reducing the molecular weight of the structural unit. In our previous works,<sup>26, 27</sup> we have firstly prepared the polytriphenylamine derivative-Poly [N,N,N, N-tetraphenylphenylenediamine] (PDDP) and poly(1-

<sup>a</sup> State Key Laboratory Breeding Base of Green Chemistry Synthesis Technology, College of Chemical Engineering, Zhejiang University of Technology, Hangzhou, 310014, P. R. China. \*E-mail: czhang@zjut.edu.cn (Cheng Zhang)

<sup>b</sup> College of Chemical Engineering, Shenyang University of Chemical Technology, Shenyang, 110142, P. R. China. \*E-mail: suchang123@hotmail.com (Chang Su)

<sup>c</sup> Hangzhou Institute of Test and Calibration for Quality and Technology Supervision, Hangzhou, 310019, P. R. China.

## ARTICLE

## Journal Name

N,1-N,4-N-triphenyl-4-N-[4-(N-[4-(N-phenylanilino)phenyl]anilineo) phenyl]benzene-1,4-diamine) (PFTP) with high free radical density structure. Specially for PDDP, it demonstrated two electron redox process with a quite high capacity of 129.1 mAh/g, as applied for the cathode material. Inspired by this, it is a promising way to further design polytriphenylamine-based derivatives for obtaining the advanced organic free radical-based cathode with high specific capacity.

In addition, the utilization ratio of the active materials in the composite electrode is another factor of affecting the specific capacity and the electrochemical performances of the electrode material. During the practical applications of the polymer-based cathode, the dense packed active materials generally hinder the contact between active sites within the organic materials and electrolyte and slow down the diffusion of  $\text{Li}^+$  in the polymer matrix during the charge/discharge process, resulting in the low utilization ratio and practical specific capacity of active materials and the decreased rate performance of lithium ion battery.<sup>28,29</sup> As presented in our experiment,<sup>27</sup> the as designed polytriphenylamine derivative-PFTP with high free radical density structure possessed a higher theoretical specific capacity of 143.7 mAh/g, but the only 74.2 mAh/g of the actual specific capacity was exhibited due to the serious aggregated morphology which decreased the utilization rate of the active material during the charge/discharge process. As an alternative, to prepare the active materials with high specific surface area will in favor of the improved contact surface of the active material with the electrolyte, allowing the more short  $\text{Li}^+$  diffusion pathways during the charge/discharge reaction and the more surface sites available for the electrochemical reaction, all of which will in turn lead to the enhanced specific capacity and kinetics.<sup>29-32</sup> Microporous conjugated polymers (MCPs), as a kind of advanced porous materials, show recently some features such as large specific surface area, high chemical and thermal stability, insolubility in most solvents, and synthetic diversity. These advantages make MCPs broad potentials in a variety of applications, such as gas adsorption, light emitting, energy storage and heterogeneous catalysis. However, there are only a few reports on applying MCPs as electrode materials of lithium ion batteries. Recently, some novel microporous organic polymers have been synthesized, such as porous polyimides,<sup>33</sup> microporous conjugated polymers based on carbazole and benzothiadiazole,<sup>34</sup> microporous conjugated polymers based on hexaazatrinaphthalene,<sup>35</sup> microporous organic polymers with triphenylamine segments<sup>36</sup> and bipolar porous polymeric frameworks with triazine structure,<sup>37</sup> et al. As employed for Li-/Na-based energy storage devices, it exhibited an unusually high specific energy and specific power. These results indicate that the high specific capacity organic electrode materials with microporous morphology have enormous potential as green sustainable and flexible electrode materials for next generation energy storage devices.

Recently, the studies have demonstrated that 4,4',4''-tris(N,N-diphenyl-amino) triphenylamine (TDATA) and its derivatives generally show excellent charge transport, and

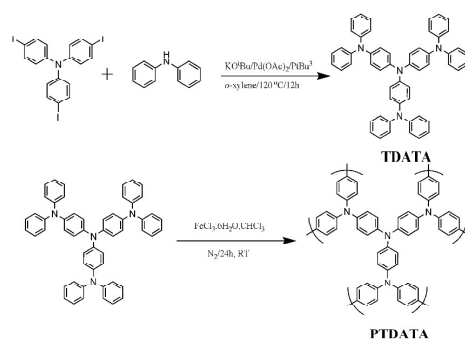
have been applied as organic electroluminescent devices and organic solar cells materials.<sup>38</sup> However, to the best of our knowledge, there are no relative reports of the corresponding polymer-PTDATA and its applications as an electro-active material in lithium ion batteries. In this study, a novel polytriphenylamine derivative (Poly(4,4',4''-tris(N,N-diphenyl-amino) triphenylamine) (PTDATA)), with a similar triphenylamine structure but an even higher free radical density than PTPA and PDDP, was prepared firstly. And then, by controlling the polymerization conditions, a novel organic mesoporous material based on the PTDATA was successfully obtained, which demonstrated a higher specific surface of 560.58  $\text{m}^2/\text{g}$  than that of 5.62  $\text{m}^2/\text{g}$  for PTPA. Furthermore, the electrochemical properties and the charge/discharge mechanism of the prepared polymer as the cathode during the charge/discharge process were systematically investigated.

## Experimental

### Material synthesis

**Materials** Diphenylamine (98%), tris(4-iodophenyl)amine (99%), *o*-xylene (99%), triphenylamine (98%), tri-tert-butylphosphine ( $\text{PtBu}_3$ , 1.0 M), Potassium tert-butoxide ( $\text{KO}_t\text{Bu}$ , 98%), and palladium acetate ( $\text{Pd}(\text{OAc})_2$ , AR) were purchased from Energy Chemical Reagent Co. All other reagents were received as analytical grade and used without further purification.

**Synthesis of TDATA monomer** 4,4',4''-tris(N,N-diphenyl-amino) triphenylamine (TDATA) was prepared by the Ullmann coupling reaction similarly as reported in literature.<sup>39,40</sup> 2 mmol of tris(4-iodophenyl)amine and 8 mmol of diphenylamine were dissolved in 50 ml *o*-xylene in a 100 ml three-necked flask, to which 0.17 g  $\text{Pd}(\text{OAc})_2$ , 1.12 g  $\text{KO}_t\text{Bu}$  and 2.4 ml  $\text{PtBu}_3$  as the catalysts were added. The mixture was stirred in a nitrogen atmosphere at 120 °C for 12 h. The final solution was extracted with  $\text{CHCl}_3$  and water. Then,  $\text{CHCl}_3$  was removed by rotary evaporation to afford the crude product. TDATA was isolated by recrystallization with THF/MeOH (1:1 v/v) mixed solvent in a 67.1 % yield as pale yellow needles.  $^1\text{H}$  NMR (500 MHz,  $\text{DMSO}-d_6$ ),  $\delta$ =7.32-7.25 (m, 12 H), 7.07-6.96 (m, 30 H) (Fig. S1 of the Supporting Information). MS (ESI): calculated  $\text{C}_{54}\text{H}_{42}\text{N}_4$  m/z: 746.4, found m/z: 746.4 (Fig. S2 of the Supporting Information).



**Scheme 1** Synthetic route of TDATA monomer and porous polymer PTDATA.

**Preparation of PTPA and meso-porous PTDATA** The polymer of poly(4,4',4''-tris(N,N-diphenyl-amino) triphenylamine) (PTDATA) and the reference polymer of poly(triphenylamine) (PTPA) were prepared by chemical oxidative polymerization in 50 mL of chloroform using ferric chloride as the oxidant. The reaction solution was stirred overnight at room temperature under N<sub>2</sub>. After completion of the solution polymerization reaction, the reaction mixture was poured into methanol to deposit the polymer product, which was then filtered and washed with methanol several times. Finally, the polymer product was filtered and dried in vacuum at 60 °C for 12 h. The colors of the PTPA and PTDATA were yellow and emerald, respectively. Synthetic routes of TDATA monomer and porous polymer PTDATA were shown in Scheme 1.

#### Material characterization

Pyrolysis-gas chromatography-mass spectrometry (PGC-MS) was carried out on a vertical microfurnace pyrolyzer (PY2020iD, Frontier Lab Ltd, Fukushima, Japan), which was directly attached to a gas chromatograph (CP-3800, Varian, USA) equipped with a flame ionization detector (FID). FT-IR spectra were carried out on a Nicolet 6700 spectrometer (Thermo Fisher Nicolet, USA) with KBr pellets. UV-Vis spectra were recorded on a UV-1800 spectrophotometer (Shimadzu, Japan). Raman spectra were recorded on a Lab RAM HR UV800 (JOBIN YVON, France) with 632.81 nm. BET was carried out on a Surface Area and Porosity Analyzer (JinWei, JW-BK122F). The electron spin resonance (ESR) spectra were recorded on BRUKER A300 spectrometer (Switzerland). Thermogravimetric analyses (TGA) were performed on a Q5000IR (Ra, USA) thermogravimetric analyzer running from room temperature to 800 °C at a heating rate of 10 °C/min in nitrogen. Scanning electron microscopy (SEM) measurements were taken using a Hitachi S-4800 scanning electron microscope (Hitachi, Japan).

#### Electrochemical measurements

For cathode characterization, CR2032 coin-type cell was used and assembled in an argon-filled glove box. The cathodic electrodes were prepared by coating a mixture containing 50 % as prepared polymers, 40 % acetylene black, 10 % PVDF binder on circular Al current collector foils, following dried at 60 °C for 10 h, and the load mass of the composite on the current collector was about 2 mg. After that, the cells were assembled with the prepared electrodes as cathode, lithium foil as the anode and 1 M LiPF<sub>6</sub> dissolved in ethylene carbonate (EC) and dimethyl carbonate (DMC) (EC/DMC = 1:1 v/v) as the electrolyte. The charge-discharge measurements were carried out on a LAND CT2001A in the voltage range of 2.5-4.2 V versus Li/Li<sup>+</sup>, using a constant current density at room temperature. Electrochemical Impedance Spectroscopy (EIS) experiments were carried out using the assembled stimulant CR2032-type coin cells of the before and after 50 charge/discharge cycles at a charge stage. And the measurements were performed with CHI 660E electrochemical working station over the frequency ranges from 0.1 Hz to 1 MHz, with the applied amplitude of 5 mV. The cyclic voltammograms (CV) tests were carried out using a CHI 660E electrochemical working station. And the testing was performed in the two-electrode electrochemical cell assembled above with the scanning potential range from 2.5 V

to 4.5 V and a scanning rate of 1 mV/s.

## Results and discussion

### Material characterization

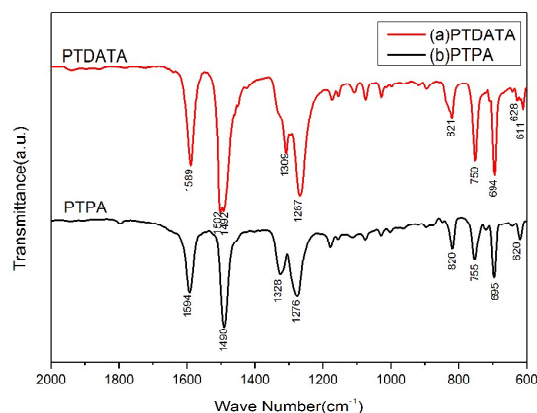


Fig. 1 FTIR spectrum of the (a) PTDATA, (b) PTPA samples.

Fig. 1 shows the FTIR spectra of the as-prepared polymers of PTDATA and PTPA, respectively. As can be seen, the main characteristic peaks of TPA can be found in Fig. 1(a) and Fig. 1(b), involving stretching vibration peak of C=C bond in benzene ring at 1594 cm<sup>-1</sup>, the C-C stretching vibration in benzene ring at 1490 cm<sup>-1</sup>, the C-H bending vibration in benzene ring at 1328 cm<sup>-1</sup> and the C-N stretching vibration in tertiary amine at 1276 cm<sup>-1</sup>, respectively. The C-H out-of-plane vibration from 1,4-disubstituted benzene rings are also shown clearly at the wavenumbers of 820 cm<sup>-1</sup>. And the presented absorption peaks at 751 and 695 cm<sup>-1</sup> are due to the C-H deformation vibration peak in substituted benzene. It is difficult to find the difference of PTDATA and PTPA on the infrared spectrum because of the similarities of the polymer structures, in which TDATA unit can be considered to be connected by three TPA molecules through the middle N atom. In order to further verify the molecular structure of the polymer, Resonance Raman spectroscopy of the as-prepared PTPA and PTDATA has also been analyzed (as shown in Fig. S3). Besides the main characteristic peaks of TPA structure in the two samples,<sup>41-43</sup> the some new bands at 1327 and 1349 cm<sup>-1</sup> appear in the spectrum of PTDATA compared to the PTPA, which are attributed to the symmetric N-Ar-Ar-N stretching and N-Ar-N stretching respectively, indicating the N-Ar-Ar-N and N-Ar-N moieties have been contained in the PTDATA polymer and the PTDATA polymer has been prepared successfully. Furthermore, the existence of radical in the products of PTPA and PTDATA is confirmed by the electron Spin resonance (ESR) (Fig. 2), in which the nearly 2 of *g* values for PTDATA (2.00562) and PTPA (2.00932) indicate the existence of the free radical in both polymers, respectively. Comparatively, the spectral intensity (*g* value: 2.00562) for PTDATA becomes more broad and strong than that of PTPA, indicative of the high free radical density in the PTDATA molecular, which is in accord with the highly free radical density structure of PTDATA molecular. The thermal stability of the PTPA and PTDATA is also investigated by thermogravimetric

## ARTICLE

analytic (TGA). And the resulted PTDATA exhibits a high thermal stability without decomposing up to 560 °C (Fig. S4 of the Supporting Information), which is crucial to the safety of rechargeable batteries.

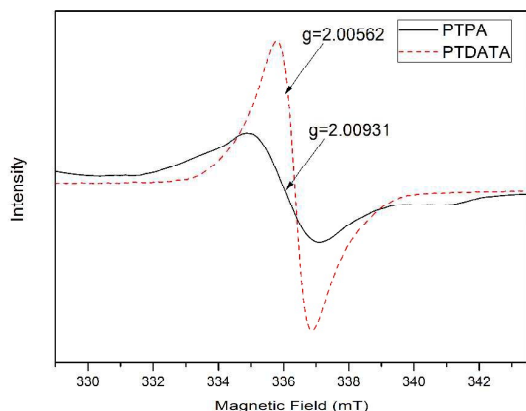


Fig. 2 ESR of PTPA and PTDATA measured in the power state.

In order to exploring the electron-structure of materials, UV-Vis spectra is further measured in DMF ( $10^{-3}$  g/L) to explore the characteristics of the monomers (TPA and TDATA) and the corresponding polymers (PTPA and PTDATA). As shown in Fig. 3(c), the TPA monomer exhibits an absorption peak at 305 nm, which are assigned to the  $\pi$ - $\pi^*$  electron transition in the TPA units. In comparison, the  $\pi$ - $\pi^*$  electron transition of TDATA monomer red-shifts to 330 nm, due to the extense  $\pi$ - $\pi^*$  conjugated structure of TDATA. After the chemical polymerization, it can be seen that the corresponding absorption peaks of the  $\pi$ - $\pi^*$  electron transition for the obtained PTPA and PTDATA become further red-shifted in comparison with that of the TPA and TDATA monomers, which can be attributed to the expansion of the  $\pi$ -conjugated structure by the produced conjugated polymer system.<sup>44, 45</sup> Still, the absorption peak of PTDATA shifts to 374 nm, which is obviously red-shift compared to PDPA (354 nm). This result indicates, due to the higher radical density structure in the repeating unit of PTDATA, that the charge carrier transportation alone in the polymer main chain of PTDATA is even smoother than that of PDPA, which is crucial for high-performance lithium battery.

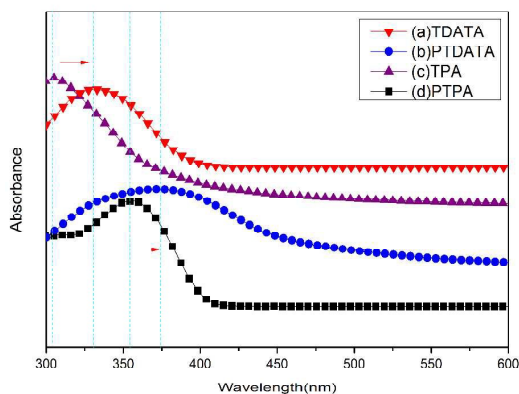


Fig. 3 UV-Vis spectra of (a) TDATA, (b) PTDATA, (c) TPA, and (d) PTPA ( $10^{-3}$  g/L) in DMF.

The morphologies of the as-obtained polymers PTPA and PTDATA have also been investigated by SEM. As can be seen in Fig. 4(a) and (c), PTPA exhibits a serious aggregated and platelike morphology with the size of several micrometers. Comparatively, the morphology of PTDATA is obviously different from that of PTPA under the same experimental conditions. As shown in Fig. 4(b) and (d), PTDATA exhibits a tangle fibrous structure with average diameter of about 20-50 nm, which forms a dense packing structure with much porous morphology in the matrix. The different morphologies can be attributed to the different molecular structures of PTDATA and PDPA, which have an effect on the molecular aggregation. Interestingly, the polytriphenylamine derivative-PFTP with the same monomer molecular formula to PTDATA shows a serious aggregated morphology, as reported in our group.<sup>27</sup> It is supposed that the differential molecular isomerism (constitutional, configurational and conformational isomers) of monomers is a possible reason for the distinct morphologies of both PTDATA and PFTP, in which the rigid molecular constitution of TDATA isomers, with less conformational isomerism, is in favour of the molecular structure stability and the obtained porous morphology of the polymer (Fig. S5 of the Supporting Information). And the much porous morphology is in favor of both electrolyte and  $\text{Li}^+$  to diffuse into the active polymer matrix, benefiting to the improvement of utilization and electrochemical properties for active materials during the charge-discharge process.

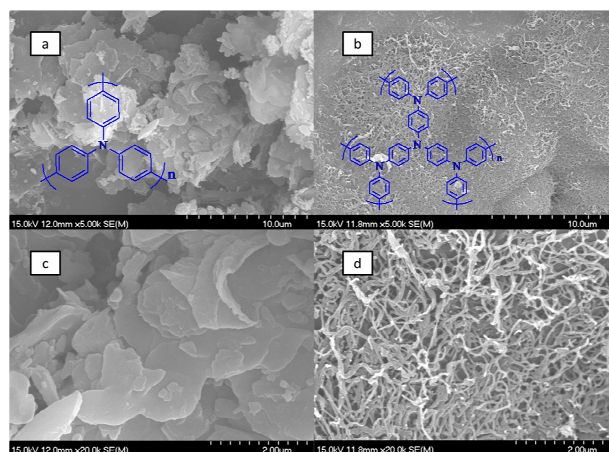


Fig. 4 SEM images (5K) of samples (a) PTPA, (b) PTDATA, (c) and (d) partially enlarged SEM images (20K) in (a) and (b), respectively.

In addition, Nitrogen adsorption/desorption isotherms and pore size distribution curves of the two polymers are shown in Fig. 5 and its inset. Two polytriphenylamine-based derivatives produced from the same polymerizations exhibits the obvious different specific surface areas ( $5.62 \text{ m}^2/\text{g}$  for PTPA and  $560.58 \text{ m}^2/\text{g}$  for PTDATA) and pore size distribution ( $\sim 10.95 \text{ nm}$  for PTPA and  $\sim 3.24 \text{ nm}$  for PTDATA), in which PTDATA shows the obviously improved structure characteristics. The rapid uptake of nitrogen of PTDATA at low relative pressures ( $P/P_0 < 0.001$ ) indicates substantial microporous structure in the polymer networks. As a sharp contrast, PTPA shows low nitrogen adsorption, which is in line with its low surface area and pore volume. A steep rise in the nitrogen adsorption isotherms for

PTDATA is also observed at high relative pressures ( $P/P_0 > 0.9$ ), indicating the presence of some mesopores and/or macropores in the polymer, which are probably due to inter-particle porosity or void. The inherent micro-/mesopore are accessible to  $\text{Li}^+$  transport and its high surface area endows PTDATA with abundant active sites for Li storage.

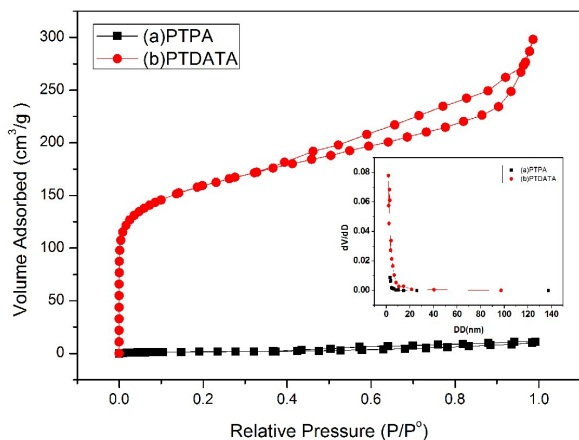


Fig. 5  $\text{N}_2$  adsorption-desorption isotherm and pore-size distribution of both PTPA and PTDATA (the inset part).

### Electrochemical performance

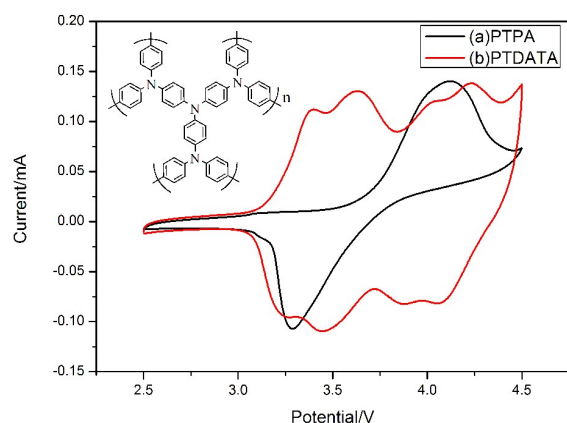
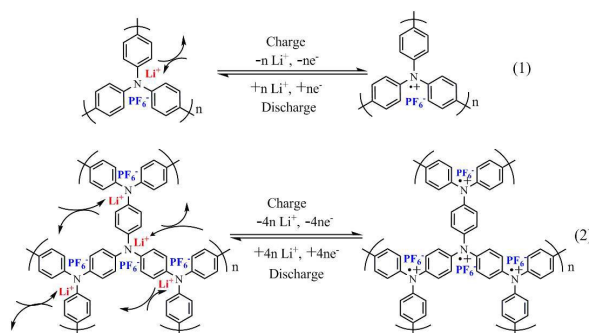


Fig. 6 Cyclic voltammograms (CV) of (a) PTPA, (b) PTDATA in the two-electrode electrochemical cell at the scan rate of 1 mV/s.

Fig. 6 shows the cyclic voltammetry (CV) profiles of the PTPA and PTDATA, which is measured using 2032 coin-type half cell at the scan rate of 1 mV/s. As shown in cyclic voltammogram (CV) profiles, the electrode of PTPA shows a pair of anodic and cathodic peaks at about 4.195 and 3.202 V respectively, according to the doping-dedoping reaction of  $\text{Li}^+$  from the polymer chains. The potential separation between the oxidation and reduction peaks is about 0.993 V, and the approximately symmetrical peaks suggest a good insertion/extraction reversibility of the produced PTPA. Comparatively, the CV curves of the PTDATA displays four pairs of oxidation and reduction peaks at 3.400 V/3.275 V, 3.636 V/3.452 V, 4.047 V/3.885 V and 4.231 V/4.059 V, respectively. The multiple peaks characteristics of PTDATA indicate the four

free radical center structure in TDATA unit of PTDATA, which undergoes the four electrons and  $\text{Li}^+$  gain/loss reaction during the charge/discharge process. And the possible reaction process for PTPA and PTDATA is shown in Scheme 2. Moreover, the potential separations for four redox pairs of PTDATA are 0.125, 0.184, 0.162 and 0.172 V, respectively, which are obviously smaller than that of PTPA, implying that the electrode polarization is small during the electrochemical oxidation/reduction process and the electrode reactivity is improved by the multi-electron reaction behaviors. It is speculated that the compact triphenylamine structure in PTDATA molecular results in higher free radical density, which will benefit the migration of the free radical electron located at the central nitrogen atom of triphenylamine moieties, as a result leading to the smaller potential separation. The result has further confirmed the obtained UV-vis spectra's results, in which the facile electron migration in the polymer is in favor of the obviously red-shifts of absorption peaks of PTDATA.



Scheme 2 The possible charge-discharge process of PTDATA, (b) PTPA samples

### Charge-discharge performance of PTDATA for Li storage

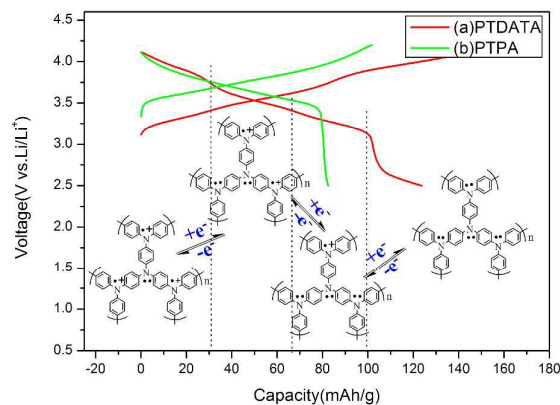
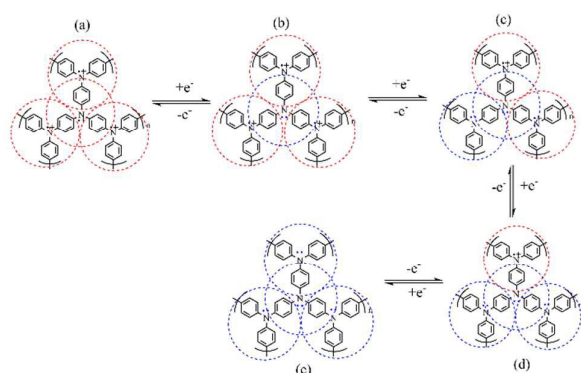


Fig. 7 Initial charge-discharge profiles of the (a) PTDATA, (b) PTPA at a constant current of 20 mA/g between 2.5 and 4.2 V in  $\text{LiPF}_6$  EC/DMC (v/v, 1:1) electrolyte versus  $\text{Li}/\text{Li}^+$ .

The charge-discharge performance in terms of lithium storage is evaluated using 2032 coin-type half cells. The initial charge-discharge profiles of two polymers at 20 mA/g between 2.5 and 4.2 V are shown in Fig. 7. As shown in Figure, PTPA shows a discharge capacity of 82.5 mAh/g at the initial cycle, with a gradually decline voltage plateau in the voltage range of 3.5-

4.1 V. In comparison, under the same conditions, the PTDATA electrode exhibits an initial discharge capacity of up to 133.1 mAh/g, which is higher than that of the measured and reported PTPA. The improved discharge capacity for PTDATA electrode can be ascribed to high theoretical capacities of PTDATA resulted by higher free radical density of TDATA unit. Furthermore, the inherent homogeneous mesoporous structure and the high specific surface area of PTDATA endow PTDATA with abundant active sites, which facilitate the contact between active sites within the organic materials and electrolyte, resulting in high utilization ratio of active materials and sequentially high practical specific capacity. Also, there exhibit four obvious voltage platforms at about 3.8, 3.4, 3.2 and 2.5 V in the discharge curve, in accord with the four redox couples observed in the CV analysis (Fig. 6). Four discharge voltage platforms contribute severally the specific capacities of 33.7 mAh/g, 35.3 mAh/g, 33.0 mAh/g and 31.1 mAh/g, and the almost equal specific capacity for the four stages indicates that equivalent status for four redox electrochemical centers during the charge/discharge process.



**Scheme 3** Schematic diagram of the possible electron donating/withdrawing effect during the four charge-discharge stages.

It is reasonable to consider that the multi-stage discharge curve characteristics of PTDATA can be attributed to the devised four-free radicals structure in the TDATA moieties of PTDATA, which exhibits a one-by-one multi-stage redox reaction process in the TDATA units during the charge/discharge process. At the first stage discharge process, three peripheral free radical cations act as the electron-withdrawing groups to the center free radical cation, which will affect the HOMO (highest occupied molecular orbital) energy level of the center radical cation and the redox potential of the active material.<sup>46</sup> As a result, PTDATA exhibits a higher discharge potential platform than that of PTPA in the initial stage of the discharge profiles of PTDATA. After the first stage discharge process, the center free radical cation in the TDATA units accepts one electron to become an electron pair, which inversely acts as an electron donating group to the remaining peripheral free radical cations, leading to that the SOMO (single occupied molecular orbital) energy level of the remaining radical cations, as well as the corresponding discharge potential plateau, decrease in the following reduction process (the second stage of the free radical discharge). And the third and the fourth discharge voltage plateaus related to the remained two free radicals are also in

the case. And the related mechanism has been illustrated in Scheme 3.

For the lithium ion battery application, the other challenging problems are the cycling stability and the rate capabilities at high charge/discharge rates. The measurement of cycling stability indicates that both the PTDATA and PTPA electrodes show a similar cycling performance (shown in Fig. 8A), namely, there is some fluctuation of capacity during the cycling process due to the nature of the organic-based material electrode. In particular, PTDATA exhibits the relatively serious capacity degradation in the initial cycles compared to PTPA, while in the following cycles its capacities maintain stable relatively, although still with some fluctuation. And after 100 cycles at a constant density of 20 mA/g, a capacity of 98.2 mAh/g can be maintained for the assembled lithium ion batteries with PTDATA as the cathode. And the relatively accepted cycling stability for the cathode materials can be attributed to the stable molecular structure of polytrienphenylamine derivatives, as well as their poor solubility in electrolyte. While, the degenerative cycling stability during the initial several charge-discharge processes can be caused by the re-aggregation behavior of the stacking mesoporous morphology of the PTDATA nanofibers, which results in the unstable cycling stability and the decreased capacity.

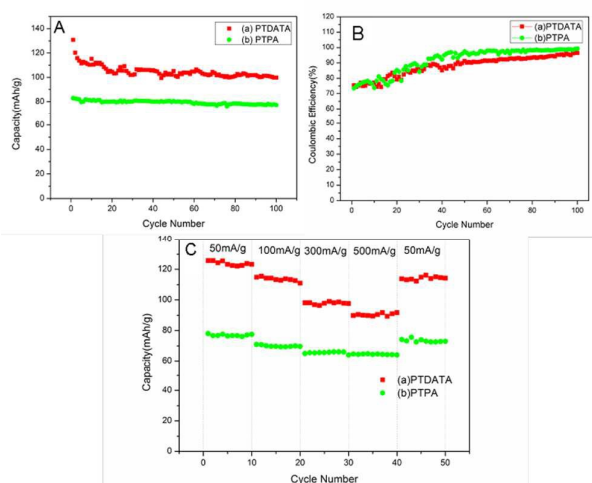


**Fig. 8** (A) Cycling stability of the (a) PTDATA, (b) PTPA at a constant current of 20 mA/g between 2.5 and 4.2 V in LiPF<sub>6</sub> EC/DMC (v/v, 1:1) electrolyte versus Li/Li<sup>+</sup>; (B) Coulombic Efficiencies of (a) PTDATA and (b) PTPA during the 100 cycles; (C) Rate performances of the polymer electrodes (a) PTDATA and (b) PTPA in the voltage range from 2.5-4.2 V at various current rates of 50, 100, 300 and 500 mA/hg.

Correspondingly, Coulombic Efficiencies (CE), which can be defined as the ratio of the discharge capacity to the charge capacity during the charging and discharging process has also been shown correspondingly in the Fig. 8B. As can be seen, both PTDATA and PTPA present the related low CE (the about 75 %) at the initial charge/discharge cycles. With the increase of the cycling process, the CE improves gradually for PTPA and PTDATA, and after the 45 cycles, the CE for PTPA reaches above 95 %. Comparatively, PTDATA demonstrates a lower CE than that of PTPA. In generally, the CE can be decided by many factors, such as the formation of SEI membrane during the charge/discharge process, the specific surface and the particle

size of the active materials, and the aggregated morphology of the active materials, the types of the corresponding anode, the electrode composites, et al. In this paper, the lower CE in the initial cycles for PTPA and PTDATA can be attributed to the gradual formation of the SEI membrane on the lithium anode; furthermore, the inferior wettability of the active materials by the electrolyte is also a possible factor for low CE in the initial cycles. And with the cycling, the most active materials are wetted through the permeation of electrolyte and the SEI membrane is gradually formed on the surface of anode, all of which results in the improved CE in the following cycling. For the lower CE of PTDATA than that of PTPA, it is considered that the high porous morphology with high specific surface can result in the unstable volume change during the repeated charge/discharge process, which may lead to the inferior CE performance of PTDATA to PTPA.

The rate capabilities of PTDATA and PTPA electrodes were further performed at various charging rates (C) of 50, 100, 300 and 500 mAh/g, respectively. Comparatively, the PTDATA electrodes show higher rate capability than that of PTPA (shown in the Fig. 8C), and with an enhanced current density at 50, 100, 300 and 500 mAh/g, PTDATA exhibits the reversible specific capacities of 125.4, 114.1, 97.5 and 90.9 mAh/g, respectively. Although the decay rate of capacity is comparatively high at high current rate, its capacity is still higher than that of PTPA, indicating the improved rate capability. In addition, PTPA and PTDATA present the ability of quickly recovered capacity, and with the further recovering the current rate to 50 mAh/g, the 74.2 and 114.4 mAh/g of specific capacity can be obtained for PTPA and PTDATA, which correspond to ~95 % and 92 % of capacity retention, respectively. The possible reasons for the improved high rate capability of PTDATA can be partly ascribed to the higher radical density structure in the repeating unit of PTDATA, which leads to that the charge carrier transportation alone in the polymer main chain of PTDATA more smooth than that of PDPA. In addition, the porous structures have been demonstrated to be beneficial for improving the rate capabilities of lithium ion batteries, and the unique structure of PTDATA with mesopores and high specific surface area is helpful for Li ion diffusion in the polymer chains, thus making PTDATA suitable as a Li storage material even at high charge/discharge rates. Thus, the PTDATA polymer might be a good potential candidate as the cathode materials for Li-based energy storage devices.

Fig. 9 shows electrochemical impedance spectra of pristine PTPA and PTDATA before and after 50 charge/discharge cycles. In these impedance plots, the initial intercept of the spectrum at the  $Z_{re}$  axis in high frequency corresponds to the resistance of the electrolyte ( $R_e$ ). The semicircle at low impedance frequencies represents the charge-transfer reaction resistance ( $R_{ct}$ ), while the straight line at low frequencies indicates the Warburg impedance ( $Z_w$ ), which displays the ion diffusion-controlled process. It can be seen in the Figure, that the  $R_e$  for the cells with both different cathode materials is almost same before or after 50 cycles, respectively, indicating that no significant change in ionic conductivity of the electrolyte or mobility of ions with the different cathode-based cell. However, it is found that  $R_e$  for the cells after 50 cycles is

slightly larger than that of the cell before 50 cycles, demonstrating an increased resistance of the electrolyte (as shown in the inset of Fig. 9). It is possible due to the formation of the SEI membrane during the charge/discharge process, which consumes the  $\text{LiPF}_6$  in the electrolyte solution, leading to the changed resistance in electrolyte after the cycling. For the charge transfer resistance ( $R_{ct}$ ), it varies with different cathodes, in which the  $R_{ct}$  for PTDATA electrode before and after 50 cycles are ~441.0 and 500  $\Omega$  and the  $R_{ct}$  for PTPA electrode before and after 50 cycles are ~1225.0 and 1400  $\Omega$ , respectively. For the each electrode material, the  $R_{ct}$  becomes large after 50 cycles, due to the intercalation of ionic species during long term cycling process<sup>47</sup> and the gradually formed SEI membrane on the surface of the electrode. While, for the different electrode materials, the small  $R_{ct}$  for PTDATA compared to PTPA indicates the fast charge transfer within PTDATA, which is of great benefit to the improved electrode kinetics. And the reduced charge transfer resistance of PTDATA may be ascribed to the delicate molecular structures and high free radical density, which led to the charge migration smoothly along polymer chain. This result is in accord with the measurement of UV-vis spectra (as displayed in the Fig. 3), in which the charge carrier transportation alone in the polymer main chain of PTDATA is even smoother than that of PDPA. In addition, the slopes of the straight lines in Nyquist plots of PTDATA is lower than that of PTPA, demonstrating that PTDATA has lower Warburg impedance and faster ion diffusion process than PTPA. These results can be attributed to the created porous morphology and the resulted high surface area, which makes the electrolyte penetration easily during the redox reaction, leading to the decrease of the charge-transfer reaction resistance.

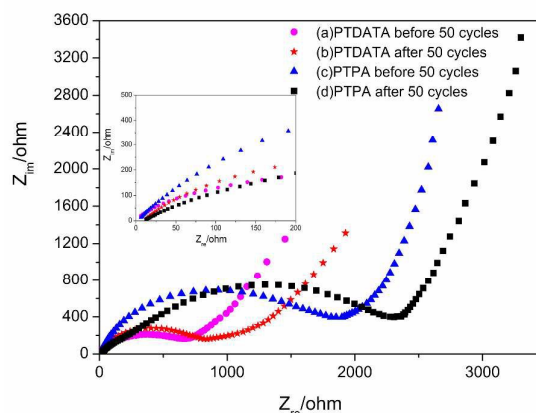


**Fig. 9** EIS of PTPA and PTDATA samples before and after 50 charge/discharge cycles in the Li/electrolyte/sample configuration. (inset: shows the partial enlarged drawing for the initial intercept of the spectrum at the  $Z_{re}$  axis in high frequency corresponds)

## Conclusions

A novel triphenylamine derivative (TDATA) with a high free radical density structure had been successfully synthesized by the Ullmann coupling reaction and the corresponding polymer (PTDATA) was then prepared by chemical oxidation polymerization, which had been demonstrated by MS, FTIR and Raman. UV-Vis spectra and EIS tests illustrated the

## ARTICLE

## Journal Name

smoother charge migration in the PTDATA polymer than in PTPA, which was attributed to the intensive free radical density structure and the improved morphology of PTDATA. PTDATA had also been firstly explored as a cathode material, in which it presented four well-defined plateaus and a quite high capacity of 133.1 mAh/g. Moreover, PTDATA exhibited an enhanced rate performance of 125.4, 114.1, 97.5 and 90.9 mAh/g with a 10 times increase of the current density from 50 to 500 mAh/g, respectively. The excellent electrochemical performances for PTDATA indicated that, for obtaining the advanced organic cathode, it was a promising way to design polytriphenylamine-based derivatives with high specific capacity and microporous structure.

### Acknowledgements

The authors gratefully thank the National Science Foundation of China (Grant No. 51573099), the Natural Science Foundation of Liaoning Province, China (Grant No.2015020441) and the National Science Foundation for Post-doctoral Scientists of China (Grant No. 2015M570524) for financial support. This work also was supported by the analysis and testing foundation of Zhejiang University of Technology.

### Notes and references

- 1 J. M. Tarascon, M. Armand, *Nature* 2001, **414**(6861), 359.
- 2 M. Armand, J. M. Tarascon, *Nature* 2008, **451**(7179), 652.
- 3 F. Y. Cheng, J. Liang, Z. L. Tao, J. Chen, *Adv. Mater.* 2011, **23**(15), 1695.
- 4 L. Taberna, S. Mitra, P. Poizot, P. Simon, J. M. Tarascon, *Nat. Mater.* 2006, **5**(7), 567.
- 5 M. Morcrette, P. Rozier, L. Dupont, E. Mugnier, L. Sannier, J. Galy, J. M. Tarascon, *Nat. Mater.* 2003, **2**(11), 755.
- 6 N. Du, H. Zhang, B. D. Chen, J. B. Wu, X. Y. Ma, Z. H. Liu, Y. Q. Zhang, D. R. Yang, X. H. Huang, J. P. Tu, *Adv. Mater.* 2007, **19**(24), 4505.
- 7 H. Li, Z. X. Wang, L. Q. Chen, X. J. Huang, *Adv. Mater.* 2009, **21**(45), 4593.
- 8 X. L. Wu, L. Y. Jiang, F. F. Cao, Y. G. Guo, L. J. Wan, *Adv. Mater.* 2009, **21**(25-26), 2710.
- 9 J. W. Park, J. Y. Eom, H. S. Kwon, *Electrochem. Commun.* 2009, **11** (3), 596.
- 10 P. Novak, K. Müller, S. V. Santhanam, O. Hass, *Chem. Rev.* 1997, **97**(1), 207.
- 11 L. X. Zhang, Z. H. Liu, G. L. Cui, L. Q. Chen, *Prog. Polym. Sci.* 2015, **43**, 136-164.
- 12 Z. P. Song, H. Zhan, Y. H. Zhou, *Angew. Chem. Int. Ed.* 2010, **49**(45), 8444.
- 13 N. Oyama, T. Tatsuma, T. Sato, T. Sotomura, *Nature* 1995, **373**(6515), 598.
- 14 M. Yao, H. Senoh, S. I. Yamazaki, Z. Siroma, T. Sakai, K. Yasuda, *J. Power Sources* 2010, **195**(24), 8336.
- 15 X. Han, C. Chang, L. Yuan, T. Sun, J. Sun, *Adv. Mater.* 2007, **19**(12), 1616.
- 16 L. G. Thierry, H. R. Kenneth, C. G. Martin, R. O. John, *J. Power Sources* 2003, **119-121**, 316.
- 17 R. H. Zeng, X. P. Li, Y. C. Qiu, W. S. Li, J. Yi, D. S. Lu, C. L. Tan, M. Q. Xu, *Electrochem. Commun.* 2010, **12**(9), 1253.
- 18 T. Suga, H. Ohshiro, S. Sugita, K. Oyaizu, H. Nishide, *Adv. Mater.* 2009, **21**(16), 1627.
- 19 K. Oyaizu, H. Nishide, *Adv. Mater.* 2009, **21**(22), 2339.
- 20 T. Suga, H. Konishi, H. Nishide, *Chem. Commun.* 2007, **17**, 1730.
- 21 J. Qu, T. Katsumata, M. Satoh, J. Wada, T. Masuda, *Polymer* 2009, **50**(2), 391.
- 22 U. Mitschke, P. Bäuerle, *J. Mater. Chem.* 2000, **10**(7), 1471.
- 23 I. K. Yakushchenko, M. G. Kaplunov, O. N. Efimov, *Phys. Chem. Chem. Phys.* 1999, **1**(8), 1783.
- 24 E. R. Mark, R. W. David, B. M. Bonnie, C. B. Bruce, *J. Mater. Chem.* 2009, **19**(38), 6977.
- 25 J. K. Feng, X. P. Ai, Y. L. Cao, H. X. Yang, *J. Power Sources* 2008, **177**(1), 199.
- 26 C. Su, F. Yang, L. L. Ji, L. H. Xu, C. Zhang, *J. Mater. Chem. A* 2014, **2**, 20083.
- 27 C. Su, L. L. Ji, L. H. Xu, N. N. Zhou, G. S. Wang, C. Zhang, *RSC Adv.* 2016, **6**, 22989.
- 28 C. Su, Y. Ye, L. Xu, C. Zhang, *J. Mater. Chem.* 2012, **22**, 22658.
- 29 C. Luo, R. Huang, R. Kevorkyants, M. Pavanello, H. He, C. Wang, *Nano. Lett.* 2014, **14**, 1596.
- 30 S. Zhang, C. Deng, H. Gao, F. L. Meng, M. Zhang, *Electrochim. Acta.* 2013, **107**, 406.
- 31 Z. Song, T. Xu, M. L. Gordin, Y. B. Jiang, I. T. Bae, Q. Xiao, H. Zhan, J. Liu, D. Wang, *Nano. Lett.* 2012, **12**, 2205.
- 32 B. L. Ellis, P. Knauth, T. Djenizian, *Adv. Mater.* 2014, **26**, 3368.
- 33 D. Tian, H. Z. Zhang, D. S. Zhang, Z. Chang, J. Han, X. P. Gao, X. H. Bu, *RSC Adv.* 2014, **4**, 7506.
- 34 S. Zhang, W. Huang, P. Hu, C. Huang, C. Shang, C. Zhang, R. Yang, G. Cui, *J. Mater. Chem. A* 2015, **3**, 1896.
- 35 F. Xu, X. Chen, Z. Tang, D. Wu, R. Fu, D. Jiang, *Chem. Commun.* 2014, **50**, 4788.
- 36 C. Zhang, X. Yang, W. Ren, Y. Wang, F. Su, J. X. Jiang, *J. Power Sources* 2016, **317**, 49.
- 37 K. Sakaushi, G. Nickerl, F. M. Wieser, D. Nishio-Hamane, E. Hosono, H. Zhou, S. Kaskel, J. Eckert, *Angew. Chem. Int. Ed.* 2012, **51**, 7850.
- 38 X. Zhou, J. Blochwitz, M. Pfeiffer, A. Nollau, T. Fritz, K. Leo, *Adv. Funct. Mater.* 2001, **11**, 310.
- 39 T. Yamamoto, M. Nishiyama, Y. Koie, *Tetrahedron Lett.* 1998, **39**, 2367.
- 40 L. Zou, Q. Peng, Y. Chen, M. Xie, *Chem. Res. Appl.* 2002, **14**, 349.
- 41 C. Kvarnström, A. Petr, P. Damlin, T. Lindfors, A. Ivaska, L. Dunsch, *J. Solid State Electrochem.* 2002, **6**(8), 505.
- 42 V. Adriana, M. E. Szeghalmi, E. Volker, S. Michael, A. Stephan, K. Volker, N. Gilbert, S. Rainer, L. Christoph, L. Dirk, S. Dietmar, Z. Manfred, P. Jürgen, *J. Am. Chem. Soc.* 2004, **126**(25), 7834.
- 43 M. Zhou, K. Wang, Z. Men, S. Gao, Z. Li, C. Sun, *Spectrochim. Acta, Part A* 2012, **97**, 526.
- 44 S. C. Hsu, W. T. Whang, C. S. Chao, *Thin Solid Films* 2007, **515**(17), 6943.
- 45 H. Cho Ko, D. K. Lim, S. Kim, W. Choi, H. Lee, *Synth. Met.* 2004, **144**(2), 177.
- 46 T. Suga, Y. Pu, S. Kasatori, H. Nishide, *Macromolecules* 2007, **40**(9), 3167.
- 47 B. Wang, Q. Liu, Z. Qian, X. Zhang, J. Wang, Z. Li, H. Yan, Z. Gao, F. Zhao, L. Liu, *J. Power Sources* 2014, **246**, 747-753.